

Sulfur-Doped Graphene as an Efficient Metal-free Cathode Catalyst for Oxygen Reduction

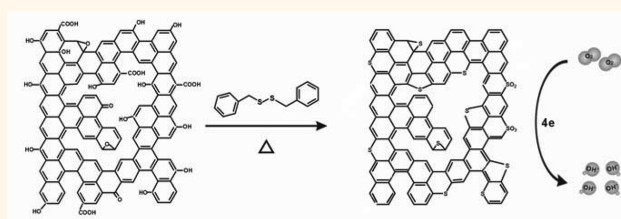
Zhi Yang,^{†,*} Zhen Yao,[†] Guifa Li,[‡] Guoyong Fang,[†] Huagui Nie,[†] Zheng Liu,[†] Xuemei Zhou,[†] Xi'an Chen,[†] and Shaoming Huang^{†,*}

[†]Nanomaterials and Chemistry Key Laboratory, Wenzhou University, Wenzhou, 325027, China and [‡]School of Material Science and Engineering, Nanchang Hangkong University, Jiangxi 330063, China

The slow kinetics of the oxygen-reduction reaction (ORR) is the major limiting factor in the energy-conversion efficiency of fuel cells (FCs).^{1,2} So far, the most effective electrocatalyst for ORRs in the cathodes of commercial FCs is Pt or its alloys.^{3,4} However, the high cost, limited supply, and poor durability of Pt have hindered the large-scale application of FCs. Numerous efforts have therefore been made to reduce or replace the Pt-based catalysts in FCs.^{5–9} In particular, the search for new nonprecious-metal catalysts (NPMCs) with high activity and practical durability for ORRs has been one of the most active fields in chemistry.⁶

Graphene, as a result of its unique two-dimensional monolayer structure of sp^2 -hybridized carbon, has attracted interest in a wide range of fields, such as electronics,^{10,11} sensors,^{12,13} batteries,^{14,15} and catalysts.¹⁶ Both theoretical calculations and detailed experiments have proven that the introduction of nitrogen (or P, B) atoms into sp^2 -hybridized carbon frameworks in graphene (or CNTs) is generally effective in modifying their electrical properties and chemical activities.¹⁷ Recent studies have confirmed that N-doped carbon materials with a graphitic structure, such as CNTs,^{5,18} graphene,^{16,19} and mesoporous graphitic arrays,²⁰ are promising candidates for replacing Pt-based catalysts for FCs, because they not only exhibit high catalytic activity, long-term stability, and excellent methanol tolerance in alkaline media, but also possess the advantages of low cost and environmental friendliness. Dai *et al.*⁵ proposed that the high activity may be attributed to the larger electronegativity of N (electronegativity of nitrogen: 3.04) with respect to C atoms (electronegativity of carbon: 2.55),²¹ and the creating of positive charge density on

ABSTRACT



Tailoring the electronic arrangement of graphene by doping is a practical strategy for producing significantly improved materials for the oxygen-reduction reaction (ORR) in fuel cells (FCs). Recent studies have proven that the carbon materials doped with the elements, which have the larger (N) or smaller (P, B) electronegative atoms than carbon such as N-doped carbon nanotubes (CNTs), P-doped graphite layers and B-doped CNTs, have also shown pronounced catalytic activity. Herein, we find that the graphenes doped with the elements, which have the similar electronegativity with carbon such as sulfur and selenium, can also exhibit better catalytic activity than the commercial Pt/C in alkaline media, indicating that these doped graphenes hold great potential for a substitute for Pt-based catalysts in FCs. The experimental results are believed to be significant because they not only give further insight into the ORR mechanism of these metal-free doped carbon materials, but also open a way to fabricate other new low-cost NPMCs with high electrocatalytic activity by a simple, economical, and scalable approach for real FC applications.

KEYWORDS: sulfur-doped graphene · nonprecious-metal catalysts · fuel cell · oxygen reduction reaction

the adjacent C atoms. These factors may result in the very favorable adsorption of O_2 . Very recently, other carbon materials doped with the low electronegative atoms such as P-doped graphite layers²² (electronegativity of phosphorus: 2.19)²¹ and B-doped CNTs²³ (electronegativity of boron: 2.04)²¹ have also shown pronounced catalytic activity. Theoretical studies using simulation calculations have confirmed that breaking the electroneutrality of graphitic materials to create charged sites favorable for O_2 adsorption is a key factor in

* Address correspondence to yang201079@126.com, smhuang@wzu.edu.cn.

Received for review September 2, 2011 and accepted December 27, 2011.

Published online December 27, 2011
10.1021/nn203393d

© 2011 American Chemical Society

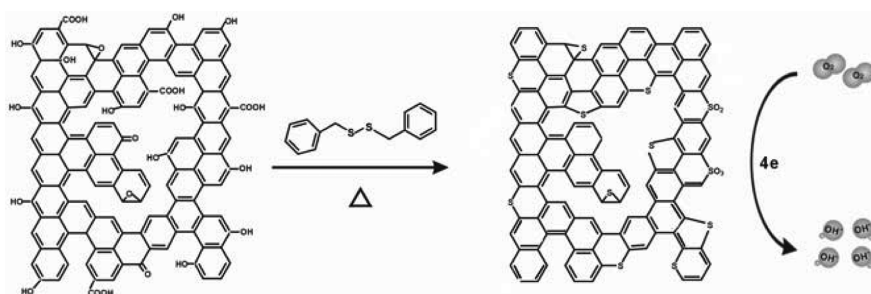


Figure 1. Schematic illustration of S-graphene preparation.

TABLE 1. Physical Parameters, Electrochemical Properties, and Corresponding Experimental Data for Various Graphenes and a Pt/C Catalyst

samples	mass ratio	specific surface	sulfide (—C—S—C—)		oxidized sulfur groups	peak potential	kinetic current density	number of electron
	Of BDS and GO	area (m ² /g)	S content (wt %)	(atom %)	(—C—S _x —C—) (atom %)	(V vs Ag/AgCl)	(mA cm ⁻²)	transfer, <i>n</i>
S-graphene-600	1:2	440	1.53	63.1	36.9	-0.32	3.07	2.51
S-graphene-900	1:2	438	1.35	70.2	29.8	-0.31	5.12	3.27
S-graphene-1050	1:2	435	1.30	82.3	17.7	-0.29	9.34	3.82
graphene-600	0	443				-0.35	1.92	1.95
graphene-900	0	437				-0.34	2.43	2.21
graphene-1050	0	436				-0.33	2.97	2.48
Pt/C							4.52	3.90

enhancing ORR activity, regardless of whether the dopants are N or B atoms.²³ Obviously, tailoring the electronic arrangement of graphene (or CNTs) by doping could be a practical strategy for producing significantly improved materials for ORRs in FCs. It will be very interesting to see what will happen when the doped element has the similar electronegativity with carbon. Sulfur (electronegativity of sulfur: 2.58) has a close electronegativity to carbon (electronegativity of carbon: 2.55).²¹ Although many investigations involving ORR catalysts based on N (or P, B) doped carbon materials have been reported, to our knowledge, sulfur-doped carbon materials have rarely been investigated.²⁴ Herein, we demonstrate the successful fabrication of sulfur-doped graphene (S-graphene) by directly annealing graphene oxide (GO) and benzyl disulfide (BDS) in argon. The electrocatalytic performances show that the S-graphenes can exhibit excellent catalytic activity, long-term stability, and high methanol tolerance in alkaline media for ORRs. Moreover, we find also that the graphenes doped with another element which has a similar electronegativity as carbon such as selenium (electronegativity of selenium: 2.55), show a similarly high ORR catalytic activity. The experimental results are believed to be significant because they not only give further insight into the ORR mechanism of these metal-free doped carbon materials, but also open a way to fabricate other new low-cost NPMCs with high electrocatalytic activity by a simple, economical, and scalable approach for real FC applications.

RESULTS AND DISCUSSION

The experimental scheme for S-graphene preparation is illustrated in Figure 1. In a typical procedure, GO and BDS were first ultrasonically dispersed in ethanol. The resulting suspension was spread onto an evaporating dish and dried at 40 °C, forming a uniform solid mixture. The mixture was placed in a quartz tube under an argon atmosphere and annealed at 600–1050 °C. The final products were collected from the quartz tube. The contents and bonding configurations of sulfur in these S-graphenes can be adjusted by varying the mass ratios of GO and BDS or the annealing temperature. For comparison, GO without any S dopant was treated under the same conditions. The resulting materials are denoted as graphene-600, S-graphene-600, graphene-900, S-graphene-900, graphene-1050, and S-graphene-1050, respectively. Their physical parameters, electrochemical properties, and corresponding experimental data are listed in Table 1.

Figure 2a shows a typical TEM image of S-graphene-1050. As can be seen from Figure 2a, transparent sheets with wrinkled and folded features are easily observed. The elemental composition analysis from the EDX pattern in Figure 2b confirmed the presence of elemental S in S-graphene-1050. The S distribution in the plane of S-graphene-1050 is relatively uniform, which is verified by STEM and the corresponding elemental mapping images (Figure 2c–g). The same C and S mappings of S-graphene-1050 suggest that not only the plane but also the edge contains S atoms.

The elemental compositions and sulfur-bonding configurations in these S-doped graphenes were further investigated using X-ray photoelectron spectroscopy (XPS) and Raman spectroscopy. The XPS spectra of GO (Figure 3a) and the graphenes (graphene-600, graphene-900, and graphene-1050, Supporting Information, Figure S1) show the presence of only carbon and oxygen atoms. The high-resolution C_{1s} spectra of GO in Figure S1b shows a new peak at approximate 286.9 eV compared to the graphenes. This result indicates that

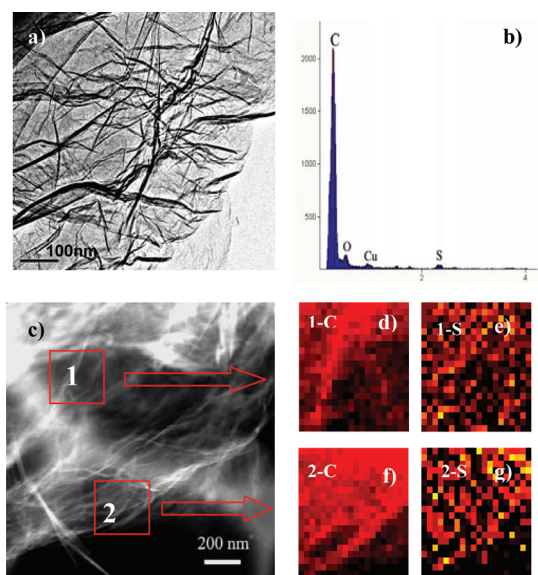


Figure 2. (a) TEM, (b) EDX, and (c) STEM images of S-graphene-1050, (d) C- and (e) S-elemental mapping of square region 1, (f) C- and (g) S-elemental mapping of square region 2.

the GO contains abundant oxygen-containing groups (e.g., carboxyl, hydroxyl, carbonyl and phenol groups).²⁵ Unlike these undoped graphenes, all the S-doped graphene samples show a visible peak corresponding to S_{2p} ; the S levels in S-graphene-600, S-graphene-900, and S-graphene-1050 are 1.53%, 1.35%, and 1.30%, respectively. This is consistent with the EDX result in Figure 2b. To clarify whether the S signals in these S-doped samples arise from physical adsorption of S or from covalent C–S bonds, all the S-graphene samples were ultrasonically dispersed in solvents such as alcohol, acetone, or H_2O . The XPS results showed no change in the S levels before and after sonication, which suggests that the covalent C–S bonds may be formed in these samples. Moreover, the previous investigations have proved that the C_{1s} peak of sp^2 carbon becomes asymmetric and broadened toward the high binding energy side as the amount of functional groups increases, rather than a single symmetry peak with a constant width.^{26–28} For the S-doped graphene, Supporting Information, Figure S1 shows that their high-resolution C_{1s} peaks corresponding to sp^2 carbon atoms up-shifted to a higher binding energy (284.7 eV) than that of pristine graphene (284.5 eV), and their full-widths at half-maximum at 284.7 eV increased with S introduction (Figure S1d). These results further suggest that GO annealing in BDS led to S incorporation into the sheets to afford C–S bonded groups. According to Kinoshita's report, some oxygen-containing groups in graphite oxide are reduced at 250–1100 °C by heat treatment.²⁶ Dai's report has confirmed the oxygen-containing groups in GO can react with NH_3 to form C–N bonds.²⁵

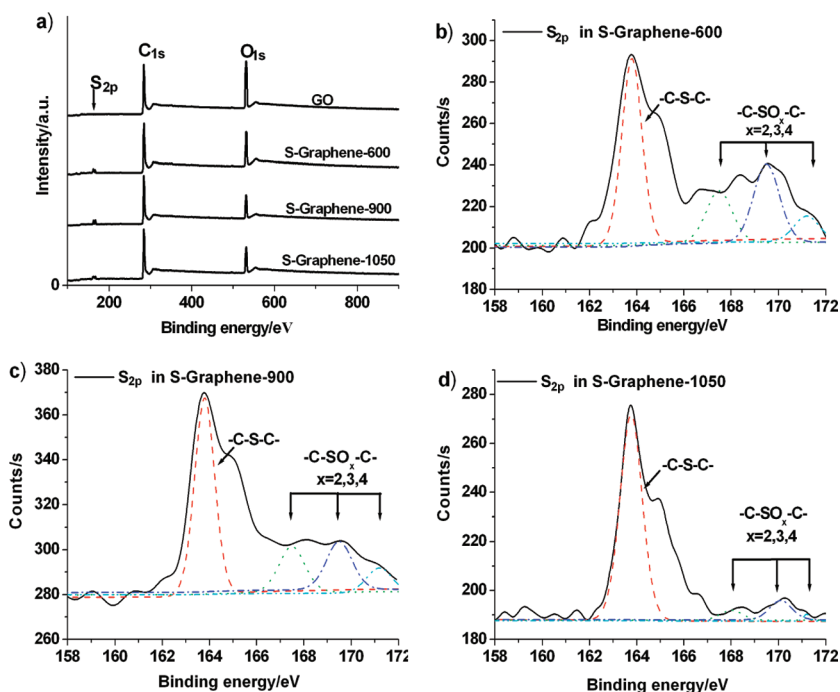


Figure 3. (a) XPS spectra of GO, S-graphene-600, S-graphene-900, and S-graphene-1050, High-resolution S_{2p} spectra of (b) S-graphene-600, (c) S-graphene-900, and (d) S-graphene-1050.

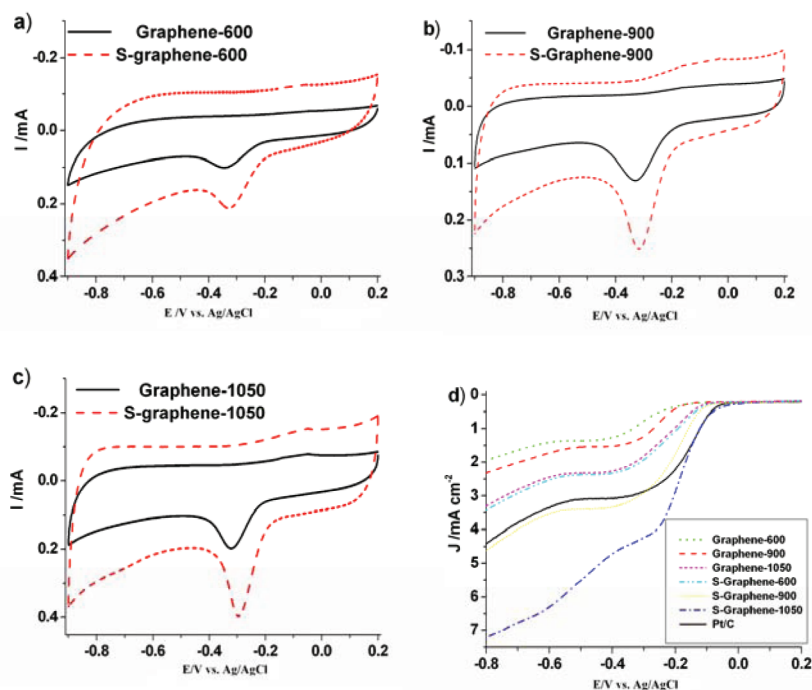


Figure 4. Cyclic voltammograms for (a) graphene-600 and S-graphene-600, (b) graphene-900 and S-graphene-900, and (c) graphene-1050 and S-graphene-1050; (d) LSV curves for various graphenes and a Pt/C catalyst on a glass carbon rotating disk electrode saturated in O_2 at a rotation rate of 1600 rpm.

Thus we speculate that the formation of a C–S bond may be attributed to the reaction between oxygen-containing groups in GO (*e.g.*, carbonyl, carboxylic, and lactone groups) and BDS. Moreover, Raman spectroscopy in Supporting Information, Figure S2 also provided direct proof for the S doping of graphene. Under similar conditions, the G peaks of the S-graphene samples down-shifted to 1580 cm^{-1} , compared to that of the pristine graphene peak at 1589 cm^{-1} ; this is an important characteristic of n-type substitutional doping of graphene.¹⁷ The similar red shift for the N-graphenes previously reported can also be observed.^{19,25} The XPS results coupled with Raman spectroscopy strongly confirmed that S atoms have been successfully introduced into the graphene framework *via* covalent bonds, and that sulfur doping of graphene can be achieved using our approach.

To investigate the electrocatalytic activities of these graphene samples, the cyclic voltammograms (CVs) in O_2 - or N_2 -saturated 0.1 M KOH solutions for different electrodes (graphene-600, S-graphene-600, graphene-900, S-graphene-900, graphene-1050, and S-graphene-1050) were measured at a constant active mass loading. The detailed information can be found in Table 1. As can be seen from Figure 4 and Supporting Information, Figure S3, distinct peaks corresponding to ORRs can be observed for all the graphene electrodes. In Figure 4a, a single cathodic reduction peak at -0.35 V can be observed in an O_2 -saturated solution for the graphene-600 electrode. After the introduction of S atoms, the peak potential of the ORR for the

S-graphene-600 electrode shifted positively to -0.32 V and its oxygen-reduction current was measured to be $123\text{ }\mu\text{A}$ after correcting background current, and was obviously higher than that of the graphene-600 electrode ($82\text{ }\mu\text{A}$). These results clearly indicate that the ORR catalytic activity of S-graphene-600 is greater than that of graphene-600. Compared with the graphene-900 electrode, the S-graphene-900 electrode also shows a slightly positive shift in the ORR peak potential, with a more pronounced increase in the ORR current (Figure 4b). Similar results can also be observed for graphene-1050 and S-graphene-1050 electrodes, as shown in Figure 4c. Our experimental results strongly approve that the S-doped graphene has a higher electrocatalytic activity than the corresponding undoped graphene. It is undoubted that the S doping plays the key role for ORR activity enhancement of graphene. Moreover, from Figure 4, it can also be found that the CVs of the S-doped graphenes show a larger background current than the corresponding undoped graphenes. We speculate that it may be attributed to the increase of the edge plane site and disorder of graphene after S-doping, resulting in improving the capacitance current.²⁹

To gain further insight into ORRs with these graphene samples, linear sweep voltammetry (LSV) measurements were performed on a rotating-disk electrode (RDE) for all of the graphene samples, and for a commercial Pt/C electrocatalyst, in O_2 -saturated 0.1 M KOH at a rotation rate of 1600 rpm. From Figure 4d, it can be seen that all of the S-graphene samples

(S-graphene-600, S-graphene-900, and S-graphene-1050) have more positive onset potentials and higher limiting current density than those of the corresponding graphenes without dopants (graphene-600, graphene-900, and graphene-1050). These results are in agreement with the CV observations, and further confirm that S introduction can significantly enhance the ORR catalytic activity of graphene. From Figure 4d, it can also be observed that the onset potential for S-graphene-1050 is close to that of the Pt/C catalyst, and that its current density (at -0.8 V) is the highest of all these materials. These results suggest that the ORR catalytic activity of S-graphene-1050 is better than that of commercial Pt/C catalysts. To further study ORRs with respect to these samples, we performed RDE measurements at various rotating speeds. The diffusion current densities depend on the rotating rates, and the number of electron transfers (n) and the kinetic-limiting current density (J_k) involved in the ORR can be calculated from the Koutecky–Levich equation (Supporting Information, Figure S5, Table 1). The n for S-graphene-1050 is calculated to be 3.82 at -0.30 V, which indicates a four-electron-transfer reaction to reduce oxygen directly to OH^- . The calculated J_k value is $9.34 \text{ mA} \cdot \text{cm}^{-2}$ at -0.30 V. The electrocatalytic activity of S-graphene-1050 can be comparable to those of N-doped CNTs (or mesoporous graphitic arrays) in an alkaline electrolyte.^{5,20} All the above results further confirm that S-graphene-1050 is a promising metal-free NPMC with high catalytic activity for ORRs.

The CV and LSV observations also show that the annealing temperature plays a very important role in the ORR catalytic activity of graphene. To further elucidate the correlations among the structures, compositions, and catalytic activities of S-graphenes obtained at different annealing temperatures, the Raman spectroscopy and XPS high-resolution results were again analyzed. As is known, the I_G/I_D value of a carbon material is an important parameter for evaluating the degree of graphitization.³⁰ From Supporting Information, Figure S2, it can be seen that the I_G/I_D values of these S-graphenes increase with increasing annealing temperature. The improved graphitic degree of the S-graphene samples might be caused by reduction effects and “self-repairing” of the graphene layer at high temperatures, and was believed to be one of the factors contributing to the significantly enhanced catalytic activity. Moreover, the binding energy of XPS- S_{2p} was also used to analyze the sulfur doping in these S-graphenes (Figure 3). Sulfur was doped into the carbon in two distinct forms: as sulfide groups ($-\text{C}-\text{S}-\text{C}-$, at ~ 163.8 eV) and as oxidized sulfur groups ($-\text{C}-\text{SO}_x-\text{C}-$, $x = 2-4$, at $167.5-171.5$ eV) such as sulfate or sulfonate.²⁹ From Figure 3b–d and Table 1, it can be seen that the oxidized sulfur groups (sulfate or sulfonate) can be transformed into sulfide groups at higher annealing temperatures. Considering

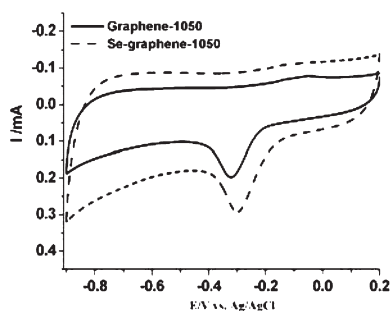


Figure 5. Cyclic voltammograms for graphene-1050 and Se-graphene-1050 in KOH solution with saturated O_2 .

the almost identical mesostructures such as surface areas (see Table 1), we speculate that the C–S bond should be an important catalytic active site for promoting ORR. According to previous reports²³ involving the origin of this ORR activity enhancement with the N (or B) doped carbon materials, breaking the electroneutrality of graphitic materials owing to the different electroneutrality between carbon and the dopant would create favorable positive charged sites for the side-on O_2 surface adsorption. This parallel diatomic adsorption could effectively weaken the O–O bonding and facilitate the direct reduction of oxygen to OH^- via a four-electron process. In our case, considering that sulfur has a close electroneutrality to carbon and the C–S bonds are predominately at the edge or the defect sites, we speculate that the change of atomic charge distribution for the S-graphene is relatively smaller, compared to N (B, or P) doped carbon materials. Very recently, Zhang *et al.* reported that the spin density should be more important in determining the catalytic active sites through using density functional theory (DFT) calculation, compared to atomic charge density.³¹ Zhang's theory may be appropriate for explaining the enhancement effect of S doping in our experiment. We believe that the spin density is the dominant factor to regulate the observed ORR activity in the S-graphene. The detailed relationship between the catalytic activity and the microstructure for the S-graphenes needs to be further investigated.

Moreover, the experimental results coupled with Zhang³¹ and Yang's reports²³ motivated us to further explore whether other dopants, which can effectively tailor spin density or atomic charge density distribution on graphene, can also enhance the ORR catalytic activity of graphene. This has been proven by the graphene doped with iodine or selenium (see Figure 5, Supporting Information, section S6, and ref 32). These experimental results are significant to further develop new NPMCs with new structure as a general rule, and make clear the ORR mechanism of doped carbon materials. We believe that more dopants may have a similar enhancement effect. The mechanism is complicated and it may be different for different dopants. The detailed mechanisms for various different dopants are under investigation.

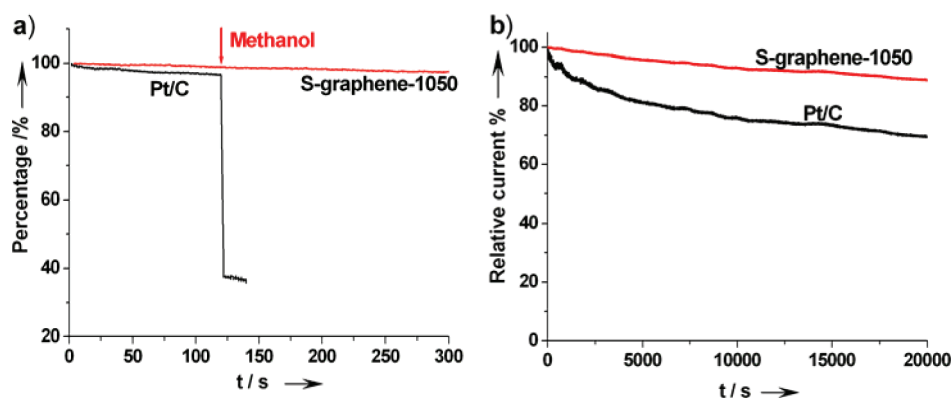


Figure 6. Chronoamperometric responses of S-graphene-1050 and Pt/C-modified GC electrodes (a) with 3 M methanol added at around 120 s and (b) at -0.30 V in an O_2 -saturated 0.1 M KOH solution.

Resistance to crossover effects and stability of the catalyst materials are important considerations for their practical application to fuel cells. The chronoamperometric responses to methanol introduced into an O_2 -saturated electrolyte were measured for S-graphene-1050 and for the Pt/C catalyst. It can be seen from Figure 6a that after the addition of 3 M methanol to a 0.1 M KOH solution saturated with O_2 , no noticeable change was observed in the ORR current at the S-graphene-1050 electrode. In contrast, the ORR current for the Pt/C catalyst decreased sharply. These results indicate that S-graphene-1050 exhibits high ORR selectivity and has a good ability for avoiding crossover effects. The durabilities of the S-graphene-1050 and Pt/C catalysts were also compared. The catalysts were held at -0.30 V for 20 000 s in an O_2 -saturated 0.1 M KOH solution. From Figure 6b, it can be

seen that the chronoamperometric response for S-graphene-1050 exhibits very slow attenuation, and a high relative current of 91.1% still persisted after 20 000 s. In contrast, the Pt/C electrode exhibits a gradual decrease, with a current loss of approximately 71.5% after 20 000 s. These results confirm that S-graphene-1050 has potential use in direct methanol and alkaline fuel cells.

In summary, we have reported a new kind of metal-free ORR catalysts, fabricated through a simple, economical, and scalable approach, which boasts a greater electrocatalytic activity than that of current commercial Pt/C catalysts. The new types of heterodoped structures may provide opportunities for further development of low-cost NPMCs with high activities and long lifetimes for practical FC applications. Our results could also provide useful information to further clarify the ORR mechanisms of doped carbon materials.

METHODS

Electrode Preparation. Glassy carbon (GC) electrodes (3 mm diameter, CH instrument Inc.) were polished with a 0.05 and 0.3 μm alumina slurry (CH Instrument Inc.) on a microcloth, and subsequently rinsed with ultrapure water and ethanol. The electrodes were then sonicated in ultrapure water, rinsed thoroughly with ultrapure water, and dried under a gentle nitrogen stream. To prepare the working electrode, all samples were ultrasonically dispersed in ethanol under the same process, and equal amounts of each catalyst were dropped onto the GC surface and dried at room temperature. For comparison, a commercially available Pt/C-modified GCE (20 wt % Pt supported on carbon black, fuel cell grade) was prepared in the same way.

Synthesis of the S-Graphene. Graphene oxide (GO) was purchased from commercial corporation. Sulfur-doped graphene (S-graphene) was synthesized by directly annealing graphene oxide (GO) and benzyl disulfide (BDS) in argon. The anneal treatment was carried out in a tube furnace with high purity argon as protective ambient. The detailed procedure is as follows: GO and BDS were first ultrasonically dispersed in ethanol for about 30 min. The resulting suspension was spread onto an evaporating dish and dried, forming a uniform solid mixture. The mixtures were placed into a quartz tube with argon atmosphere and annealed at 600–1050 $^{\circ}\text{C}$. After that, the sample was cooled to room temperature under ambient Ar and collected from the quartz tube. The contents and bonding configurations of sulfur in these S-graphenes can be adjusted through varying the mass ratio of GO and BDS as well as the annealing

temperatures. The graphenes doped with selenium were synthesized by directly annealing graphene oxide (GO) and diphenyl diselenide in argon. For comparison, the GO without any dopants was treated under the same condition. The resulting materials are denoted as graphene-600, S-graphene-600, graphene-900, S-graphene-900, graphene-1050, S-graphene-1050, l-graphene-1050, and Se-graphene-1050, respectively. Their physical parameters, electrochemical properties, and corresponding experimental data are listed in Supporting Information, Table S1.

Electrochemical Measurements. All electrochemical measurements, including cyclic voltammograms (CV), rotating-disk electrode voltammograms and chronoamperometry, were performed at room temperature in 0.1 M KOH solutions, which were purged with high purity nitrogen or oxygen for at least 30 min prior to each measurement.

Characterizations of Physical Parameters. X-ray photoelectron spectroscopy (XPS) measurements were carried out with an ultrahigh vacuum setup, equipped with a monochromatic Al K α X-ray source and a high resolution Gammadata-Scienta SES 2002 analyzer. Transmission electron microscopy (TEM) and high-resolution transmission electron microscopy (HRTEM) images were recorded with a JEOL-3010 instrument. The specific surface area was calculated using the Brunauer–Emmett–Teller (BET) equation. The nitrogen adsorption/desorption data were recorded at the liquid nitrogen temperature (77 K) using a Micromeritics ASAP 2020 M apparatus. Before the measurements, the samples were evacuated for 10 h at 300 $^{\circ}\text{C}$.

Acknowledgment. The work was supported in part by grants from NSFC (51002106, 21005055, 21173259) and NSFC for Distinguished Young Scholars (51025207), BSTWZ (G20100191), NSFZJ (R4090137, Y4100520) and ZJED Innovative Team for S. Huang.

Supporting Information Available: XPS spectra, Raman, CV, and LSV results for GO, graphenes, S-graphenes, and Se-graphenes. This material is available free of charge via the Internet at <http://pubs.acs.org>.

REFERENCES AND NOTES

- Xiong, W.; Du, F.; Liu, Y.; Perez, A.; Supp, M.; Ramakrishnan, T. S.; Dai, L. M.; Jiang, L. 3-D Carbon Nanotube Structures Used as High Performance Catalyst for Oxygen Reduction Reaction. *J. Am. Chem. Soc.* **2010**, *132*, 15839–15841.
- Snyder, J.; Fujita, T.; Chen, M. W.; Eeleancher, J. Oxygen Reduction in Nanoporous Metal–Ionic Liquid Composite Electrocatalysts. *Nat. Mater.* **2010**, *9*, 904–907.
- Lim, B.; Jiang, M. J. P.; Cho, E. C.; Tao, J.; Lu, X. M.; Zhu, Y. M.; Xia, Y. N. Pd–Pt Bimetallic Nanodendrites with High Activity for Oxygen Reduction. *Science* **2009**, *324*, 1302–1305.
- Chen, Z. W.; Waje, M.; Li, W. Z.; Yan, Y. S. Supportless Pt and PtPd Nanotubes as Electrocatalysts for Oxygen-Reduction Reactions. *Angew. Chem. Int. Ed.* **2007**, *46*, 4060–4063.
- Gong, K. P.; Du, F.; Xia, Z. H.; Durstock, M.; Dai, L. M. Nitrogen-Doped Carbon Nanotube Arrays with High Electrocatalytic Activity for Oxygen. *Science* **2009**, *323*, 760–764.
- Serov, A.; Kwak, C. Review of Non-platinum Anode Catalysts for DMFC and PEMFC Application. *Appl. Catal. B: Environ.* **2009**, *90*, 313–320.
- Bashyam, R.; Zelenay, P. A Class of Non-precious Metal Composite Catalysts for Fuel Cells. *Nature* **2006**, *443*, 63–66.
- Zhang, J.; Sasaki, K.; Sutter, E.; Adzic, R. R. Stabilization of Platinum Oxygen-Reduction Electrocatalysts Using Gold Clusters. *Science* **2007**, *315*, 220–224.
- Sun, Y. Q.; Li, C.; Xu, Y. X.; Bai, H.; Yao, Z. Y.; Shi, G. Q. Chemically Converted Graphene as Substrate for Immobilizing and Enhancing the Activity of a Polymeric Catalyst. *Chem. Commun.* **2010**, *46*, 4740–4742.
- Li, X. L.; Zhang, G. Y.; Bai, X. D.; Sun, X. M.; Wang, X. R.; Wang, E.; Dai, H. J. Highly Conducting Graphene Sheets and Langmuir Blodgett Films. *Nat. Nanotechnol.* **2008**, *3*, 538–542.
- Lee, C.; Wei, X.; Kysar, J. W.; Hone, J. Measurement of the Elastic Properties and Intrinsic Strength of Monolayer Graphene. *Science* **2008**, *321*, 385–389.
- Patil, A. J.; Vickery, J. L.; Scott, T. B.; Mann, S. Aqueous Stabilization and Self-Assembly of Graphene Sheets into Layered Bio-nanocomposites Using DNA. *Adv. Mater.* **2009**, *21*, 3159–3164.
- Lu, C. H.; Yang, H. H.; Zhu, C. L.; Chen, X.; Chen, G. N. A Graphene Platform for Sensing Biomolecules. *Angew. Chem., Int. Ed.* **2009**, *48*, 4785–4787.
- Wu, Z. S.; Ren, W. C.; Xu, L.; Li, F.; Cheng, H. M. Doped Graphene Sheets as Anode Materials with Superhigh Rate and Large Capacity for Lithium Ion Batteries. *ACS Nano* **2011**, *5*, 5463–5471.
- Yoo, E.; Kim, J.; Hosono, E.; Zhou, H.; Kudo, T.; Honma, I. Enhanced Cyclic Performance and Lithium Storage Capacity of SnO₂/Graphene Nanoporous Electrodes with Three-Dimensionally Delaminated Flexible Structure. *Nano Lett* **2008**, *8*, 2277–2282.
- Qu, L. T.; Liu, Y.; Baek, J. B.; Dai, L. M. Nitrogen-Doped Graphene as Efficient Metal-free Electrocatalyst for Oxygen Reduction in Fuel Cells. *ACS Nano* **2010**, *4*, 1321–1326.
- Liu, H. T.; Liu, Y. Q.; Zhu, D. B. Chemical Doping of Graphene. *J. Mater. Chem.* **2011**, *21*, 3335–3345.
- Yu, S. S.; Zhang, Q.; Dai, L. M. Highly Efficient Metal-free Growth of Nitrogen-Doped Single-Walled Carbon Nanotubes on Plasma-Etched Substrates for Oxygen Reduction. *J. Am. Chem. Soc.* **2010**, *132*, 15127–15129.
- Sheng, Z. H.; Tao, L.; Chen, J. J.; Bao, W. J.; Wang, F. B.; Xia, X. H. Catalyst-free Synthesis of Nitrogen-Doped Graphene via Thermal Annealing Graphite Oxide with Melamine and Its Excellent Electrocatalysis. *ACS Nano* **2011**, *5*, 4350–4358.
- Liu, R. L.; Wu, D. Q.; Feng, X. L.; Mullen, K. Nitrogen-Doped Ordered Mesoporous Graphitic Arrays with High Electrocatalytic Activity for Oxygen Reduction. *Angew. Chem., Int. Ed.* **2010**, *49*, 2565–2569.
- Lide, D. R. *CRC Handbook of Chemistry and Physics*, 84th ed.; CRC Press: Boca Raton, FL, 2003.
- Liu, Z. W.; Peng, F.; Wang, H. J.; Yu, H.; Zheng, W. X.; Yang, J. Phosphorus-Doped Graphite Layers with High Electrocatalytic Activity for the O₂ Reduction in an Alkaline Medium. *Angew. Chem., Int. Ed.* **2011**, *50*, 3257–3261.
- Yang, L.; Jiang, S. J.; Yu, Y.; Zhu, L.; Chen, S.; Wang, X. Z.; Wu, Q.; Ma, J.; Ma, Y. W.; Hu, Z. Boron-Doped Carbon Nanotubes as Metal-free Electrocatalysts for the Oxygen Reduction Reaction. *Angew. Chem., Int. Ed.* **2011**, *50*, 7132–7135.
- Paraknowitsch, J. P.; Thomas, A.; Schmidt, J. Microporous Sulfur-Doped Carbon from Thienyl-Based Polymer Network Precursors. *Chem. Commun.* **2011**, *47*, 8283–8285.
- Li, X. L.; Wang, H. L.; Robinson, J. T.; Sanchez, H.; Diankov, G.; Dai, H. J. Simultaneous Nitrogen Doping and Reduction of Graphene Oxide. *J. Am. Chem. Soc.* **2009**, *131*, 15939–15944.
- Kinoshita, K. *Carbon: Electrochemical and Physicochemical Properties*; Wiley: New York, 1988.
- Lerf, A.; He, H. Y.; Forster, M.; Klinowski, J. Structure of Graphite Oxide Revisited. *J. Phys. Chem. B* **1998**, *102*, 4477–4482.
- Gao, W.; Alemany, L. B.; Ci, L. J.; Ajayan, P. M. New Insights into the Structure and Reduction of Graphite Oxide. *Nat. Chem* **2009**, *1*, 403–408.
- Choi, C. H.; Park, S. H.; Woo, S. I. Heteroatom Doped Carbons Prepared by the Pyrolysis of Bio-derived Amino Acids as Highly Active Catalysts for Oxygen Electro-reduction Reactions. *Green Chem.* **2011**, *13*, 406–412.
- Das, A.; Pisana, S.; Chakraborty, B.; Piscac, S.; Saha, S. K.; Waghmare, U. V.; Novoselov, K. S.; Krishnamurthy, H. R.; Geim, A. K.; Ferrari, A. C. Monitoring Dopants by Raman Scattering in an Electrochemically Top-Gated Graphene Transistor. *Nat. Nanotechnol.* **2008**, *3*, 210–215.
- Zhang, L. P.; Xia, Z. H. Mechanisms of Oxygen Reduction Reaction on Nitrogen-Doped Graphene for Fuel Cells. *J. Phys. Chem. C* **2011**, *115*, 11170–11176.
- Yao, Z.; Nie, H. G.; Yang, Z.; Zhou, X. M.; Liu, Z.; Huang, S. M. Catalyst-Free Synthesis of Iodine-Doped Graphene via a Facile Thermal Annealing Process and Its Use for Electrocatalytic Oxygen Reduction in an Alkaline Medium. *Chem. Commun.* **2012**, DOI: 10.1039/C2CC16192C.